

## Effect of Diluent on Molecular Motion and Glass Transition in Polymers. IV. The System Poly(methyl acrylate)—Toluene

Keiichiro ADACHI and Yoichi ISHIDA

*Department of Polymer Science, Faculty of Science,  
Osaka University, Toyonaka, Osaka 560, Japan.*

(Received May 25, 1978)

**ABSTRACT:** The influences of diluent on molecular motions and glass transition were studied on the system poly(methyl acrylate)—toluene by means of dielectric and thermal measurements over a wide concentration range. Three relaxation processes assigned respectively to the segmental motion of the polymer chain, rotation of the side group, and local motion were recognized between 80 and 300K with decreasing temperature. Two step-wise changes in DTA diagram were observed and can be assigned as glass transition points  $T_{gI}$  and  $T_{gII}$ . The magnitude of dielectric dispersion, activation plot, and glass transition temperature are discussed by comparing them with those of systems reported previously. Coalescence of the primary and secondary loss peaks was observed and are explained in terms of the correlation functions for motion of the dipole.

**KEY WORD** Poly(methyl acrylate) / Dielectric Relaxation / Glass Transition / Concentrated Solution / Diluent Effect /

We have recently investigated dielectric relaxation and glass transition in concentrated solutions of amorphous polymers over a wide range of concentration and temperature.<sup>1-3</sup> These investigations revealed the common features of concentrated solutions in regard to the following three points, *i. e.*, (1) classification of relaxation processes, (2) relationship between glass transition point and dielectric relaxation, and (3) concentration dependences of the activation plot and magnitude of dispersion for primary relaxation process. In this study, we measured the complex dielectric constant and glass transition temperature on the system poly(methyl acrylate)—toluene in order to compare the behavior of this system with those of the systems reported previously, in terms of the features mentioned above.

It is known that poly(methyl acrylate) shows a marked dielectric secondary relaxation associated with the rotation of the side group at about 180 K in a bulk state.<sup>4</sup> Since some data have been reported concerning the effect of diluent on mobility of a side group,<sup>3,5</sup> our aim is also to study the influence of diluent on the motion of the side group.

### EXPERIMENTAL

Poly(methyl acrylate) (PMA) was prepared by polymerizing methyl acrylate with use of azobisisobutyronitrile as the initiator. The polymer was purified by repeated dissolution and precipitation with benzene and methanol. The molecular weight of the PMA determined from the intrinsic viscosity was  $1.4 \times 10^6$ . Toluene (TOL), of spectrally pure grade, was used after being dried with metallic sodium. Dielectric measurements between 25 Hz and 100 kHz were carried out with a capacitance bridge (General Radio, 1615-A), but from 1 to 150 MHz, measurements were carried out with a twin T bridge (Fujisoku, DLB-1101 D). The automatic capacitance bridge (Yokogawa-Hewlett-Packard, 4270-A) was also used for measurements at 1, 10, 100, and 1000 kHz. The study of differential thermal analysis was performed with a heating rate of about 5°C/min. Details of the dielectric and thermal measurements have been described elsewhere.<sup>1,6</sup>

## RESULTS AND DISCUSSIONS

*Assignment of Relaxation Processes*

Representative temperature dependence curves of the dielectric constant  $\epsilon'$  and loss factor  $\epsilon''$  for the solutions with concentrations of 30 and 60% by weight are shown in Figures 1 and 2. Three loss peaks are recognized between 80 and 300K, as in the system of polystyrene (PS)—TOL<sup>1</sup> and poly(vinyl acetate) (PVAC)—TOL.<sup>3</sup> We designate these relaxation processes as  $\alpha$ ,  $\beta$ , and  $\gamma$  in order of decreasing temperature. Figure 3 shows concentration dependence of the loss-peak temperatures at 1 kHz for these processes. As is shown in Figures 1 and 2, the  $\gamma$  loss-peak was observed only as a shoulder. Therefore the loss-peak temperature for the  $\gamma$  process was estimated by resolving the loss curve into the  $\beta$  and  $\gamma$  loss peaks in the manner that two loss peaks have an appro-

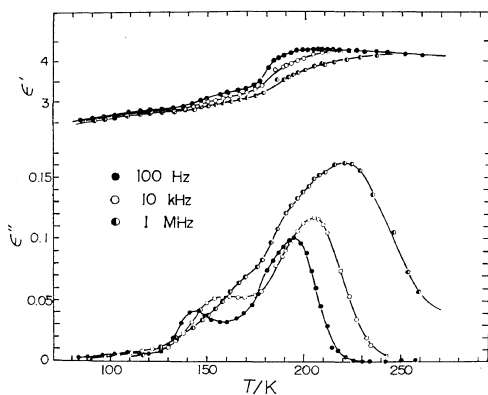


Figure 1. Temperature dependence of  $\epsilon'$  and  $\epsilon''$ , concentration 30%.

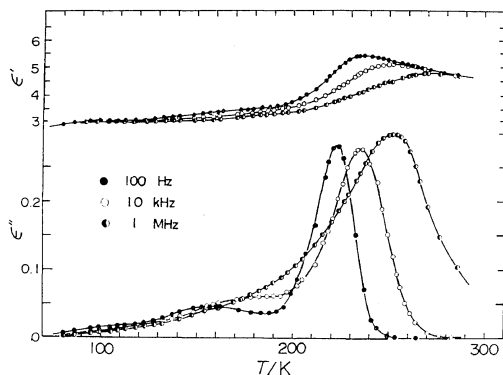


Figure 2. Temperature dependence of  $\epsilon'$  and  $\epsilon''$ , concentration 60%.

priate shape. Since the peak temperatures for the  $\alpha$  and  $\beta$  processes correspond well to those of the primary and secondary relaxations of the bulk PMA, the  $\alpha$  and  $\beta$  processes in high concentration range can be ascribed respectively to segmental motion of the PMA and the motion of the side group. However it can not be concluded that the  $\beta$  process in the solution of lower concentration is attributable to the motion of the side group since the secondary loss peak of the systems PS—TOL and PVAC—TOL was confirmed to be the motion of the solvent by combined use of NMR.<sup>1,3</sup> In Figure 4, the  $\beta$  loss peaks at 100 Hz for the solutions of various concentrations are shown. Since the motion of toluene also causes dielectric relaxation at about 130K, it may be expected that the loss peak due to the rotation of toluene appears also in the present system around this temperature region. However, as is shown in Figure 4, one

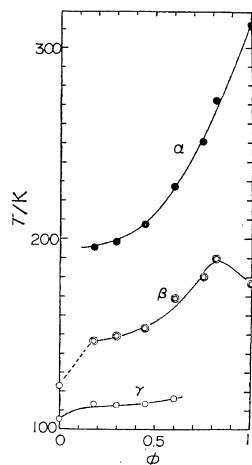


Figure 3. Concentration dependence of loss-peak temperatures at 1 kHz.  $\phi$  denotes weight fraction of the PMA. The plots at zero concentration correspond to the primary and secondary loss peaks of toluene.

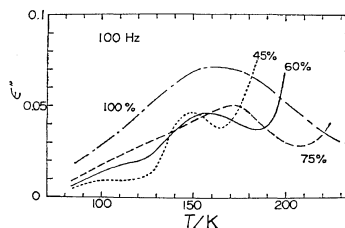
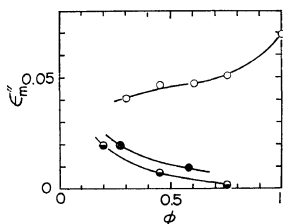


Figure 4. Temperature dependences of  $\epsilon''$  in the  $\beta$  region for the solutions of various concentrations.



**Figure 5.** Concentration dependences of the maximum values of  $\epsilon''$  for the secondary loss peak:  $\circ$ , PMA—TOL;  $\bullet$ , PVAC—TOL;  $\ominus$ , PS—TOL.

cannot distinguish these peaks due to motions of the side group and the solvent separately. Since the side group has a much larger dipole moment than toluene, the loss peak of TOL might not be appreciable. As can be seen in Figure 5, the maximum value of loss factor for the  $\beta$  process increases with concentration in contrast to the behavior noted in the PS—TOL and the PVAC—TOL systems.<sup>1,3</sup> This fact gives an evidence for the conclusion that the loss peak of the  $\beta$  process is due mainly to the motion of the side group.

The effect of diluents on the mobility of the side group was studied by Mikhailov, *et al.*,<sup>5</sup> who carried out dielectric measurement on the system poly(methyl methacrylate)—dibutylphthalate above 75-% concentration. They concluded that the loss peak for motion of the side group was not influenced by the diluent. On the other hand, the peak temperature of the  $\beta$  process in the present system depends moderately on concentration as can be seen in Figure 3. It is interesting that above an 80-% concentration, the loss peak temperature

for the  $\beta$  process decreased with increasing concentration. The tentative explanation for this fact is as follows. When the solvent is introduced into the bulk polymer, the free space for the rotational motion of the side group might be occupied by the solvent and hence the motion of the side group suffers greater hindrance than in the bulk state. It is also recognized that the shape of the loss curve varies with concentration as is seen in Figure 4. Therefore, we may conclude that the diluent influences the mobility of the side group although the effect is moderate. On the other hand, the  $\gamma$  process undergoes only a slight influence by the diluent, as in the other systems.<sup>1-3</sup> Thus, the  $\gamma$  process can be assigned as the so-called local motion.<sup>4</sup>

#### Magnitude of Dispersion

The frequency dependence of the dielectric loss factors are shown in Figures 6, 7, and 8 for concentrations 45, 75, and 100% by weight, respectively. With increasing temperature, the  $\alpha$  and  $\beta$  peaks coalesce as is shown in these figures. The Cole-Cole plots depicted from these data have the shape of two arcs partially overlapping. By resolving the plot into two arcs, we determined the magnitudes of dispersion for the  $\alpha$  process  $\Delta\epsilon_\alpha$  and that for the  $\beta$  process  $\Delta\epsilon_\beta$ . They are listed in Table I where the values of the effective dipole moments calculated from Onsager's equation are also listed. It is noted that the dipole moments thus determined are the values above the glass transition point ( $T_{gI}$  discussed later). As can be recognized from the table, the effective dipole moment per monomeric unit for the  $\alpha$  process

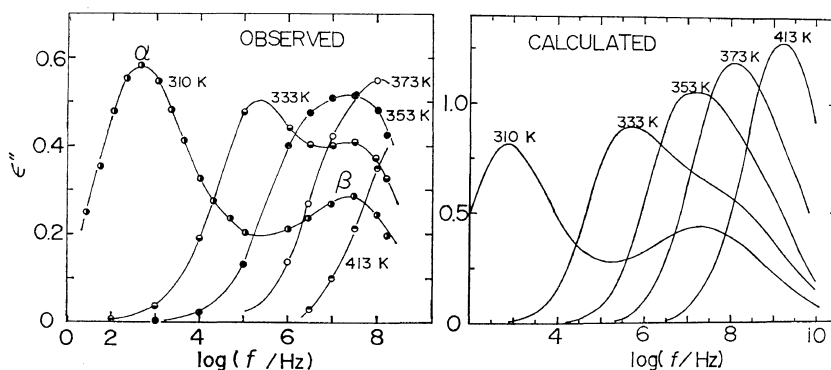


**Figure 6.** Frequency dependences of  $\epsilon''$  observed (left side) and calculated in terms of transformation of eq 8 for the 45-% solution.

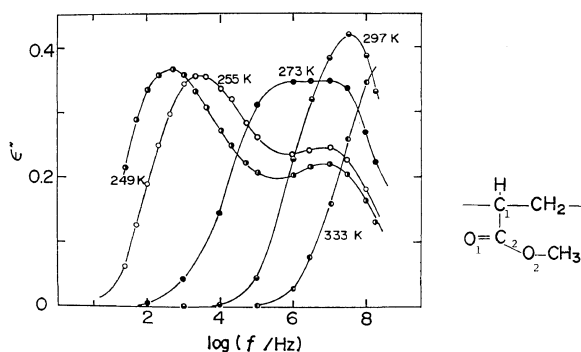


Figure 7. Frequency dependence of  $\epsilon''$ , concentration 75%.

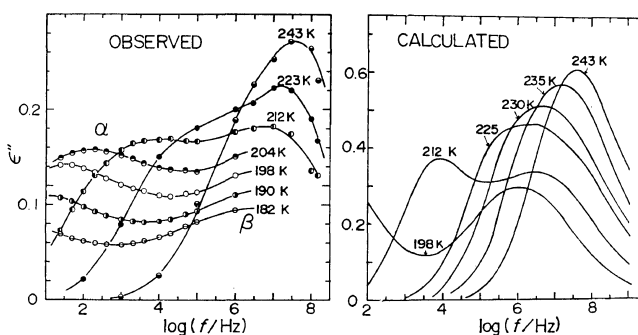


Figure 8. Frequency dependences of  $\epsilon''$  observed (left side) and calculated (right side) for the bulk PMA.

Table I. Magnitude of dispersions, effective dipole moments in Debye unit, and the parameters of eq 4

Weight fraction	$T^a$ , K	$\Delta\epsilon_\alpha$	$\mu_\beta$ , D	$\Delta\epsilon_\alpha$	$\mu_\beta$ , D	$A$	$B$	$T_0$ , K
0.45	212	1.1	0.79	1.3	1.0			
0.45	145			0.39	0.43			
0.60	226	2.1	0.92	1.7	1.0	15.1	906	152.5
0.60	155			0.50	0.44			
0.75	249	2.1	0.94	1.8	1.0	13.0	601	191.8
0.75	170			0.58	0.44			
1.00	309	2.6	0.77	1.9	0.9	13.0	670	243.8
1.00	160			0.86	0.39			

<sup>a</sup>  $T$  denotes temperatures at which  $\Delta\epsilon$  and  $\mu$  are determined.

$\mu_\alpha$  has a maximum in the range of concentration from 50 to 70%. A similar tendency of the dipole moment for the primary process is found for other systems reported previously. Thus, this tendency may be a typical feature of concentrated solutions of amorphous polymer. The effective dipole moment for the  $\beta$  process  $\mu_\beta$  above  $T_{gI}$  is almost independent of concentration. For the sake of

comparison,  $\Delta\epsilon_\beta$  below  $T_{gI}$  was also determined from the temperature dependence curve of  $\epsilon''$  based on the relation given by

$$\Delta\epsilon = (2E/R) \int_0^\infty \epsilon'' d(1/T) \quad (1)$$

where  $E$ ,  $R$ , and  $T$  denote respectively the activation energy, gas constant, and absolute tempera-

ture.<sup>4</sup> As can be seen in Table I, the value of  $\Delta\epsilon_\beta$  below  $T_{g1}$  is remarkably smaller than those above  $T_{g1}$ . The motion of the side group in the glassy state is more restricted than that above  $T_{g1}$ , as discussed below.

The molecular structure of PMA is shown in the margin of Figure 7. Since the bond  $C_2=O_1$  has a dominant bond moment, the value of  $\mu_\beta$  is determined by the amplitude ( $\theta/2$ ) of rotational motion of the side group around the bond  $C_1-C_2$ . The dipole moment of the side group can be resolved into two components. One is parallel to the bond  $C_1-C_2$  ( $\mu_1$ ) and the other is that component at right angles to the bond ( $\mu_2$ ). It was reported that the dipole moment of the ester group is 1.67 D and that the angle between the direction of the dipole and the bond  $C_1-C_2$  is  $70^\circ$ .<sup>7</sup> From this data we can deduce the values of  $\mu_1$  and  $\mu_2$  to be 0.57 and 1.57 D respectively. Obviously  $\mu_1$  does not change direction when the side group rotates and hence contributes to the dispersion of the  $\alpha$  process. The values of  $\mu_1$  and  $\mu_2$  differ appreciably from the values of  $\mu_\alpha$  and  $\mu_\beta$ . This must be a result of restriction for free rotation of the side group. Two kinds of the restrictions may be considered. One arises from a stereo-hindrance which restricts the range of angle allowed to rotate. The other is the hindrance by potential energy  $\Delta G$  in the allowed range of angle for the rotational motion. When the side group can move freely in the range of angle between  $0^\circ$  and  $\theta^\circ$  around  $C_1-C_2$ , the contribution of  $\mu_2$  to  $\Delta\epsilon_\alpha$  and to  $\Delta\epsilon_\beta$  are proportional to  $\mu_2^2 \cos^2(\theta/2)$  and  $\mu_2^2 \sin^2(\theta/2)$ , respectively. Therefore the ratio of  $\Delta\epsilon_\alpha$  to  $\Delta\epsilon_\beta$  is given approximately by

$$\Delta\epsilon_\alpha/\Delta\epsilon_\beta = (\mu_1^2 + \mu_2^2 \cos^2(\theta/2)) / \mu_2^2 \sin^2(\theta/2) \quad (2)$$

Restriction of the latter type is represented by the site model.<sup>4</sup> If one assumes that the side group changes its orientation by hopping between two sites with an energy difference  $\Delta G$ ,  $\Delta\epsilon_\beta$  is expressed by

$$\Delta\epsilon_\beta = [(4\pi N\mu^2)/(3kT)](F/E)[4K/(1+K)^2] \quad (3)$$

where  $N$ ,  $\mu$ ,  $K$ , and  $(F/E)$  represent respectively number of the dipole,  $\mu_2 \cos(\theta/2)$ ,  $\exp(-\Delta G/RT)$ , and the ratio of internal field to applied field. If it is assumed that the motion of the side group is restricted by the former type alone, the values of  $\theta$  come to  $103^\circ$  and  $87^\circ$  for the 45-% solution and

the bulk PMA, respectively. The value of  $\Delta\epsilon_\beta$  depends strongly on temperature as is shown in Table I. This dependence can be explained by the restriction of the latter type. Although we have no foundation for assuming that there exists two sites, we can estimate the order of the energy difference using eq 2. The value of  $\Delta G$  amounts to 4.6 kJ/mol for the 45-% solution whereas it is 2.2 kJ/mol for the bulk PMA. Thus, the diluent affects the motion of the side group so that the angle  $\theta$  is widened while the energy difference  $\Delta G$  is increased.

#### Concentration Dependence of Activation Plots

As is shown in Figure 9, the activation plots for the  $\alpha$  process are not linear. We have examined whether the plots conform to the Vogel—Tamman equation given by<sup>8,9</sup>

$$\log f_m = A - B/(T - T_0) \quad (4)$$

where  $f_m$  denotes the frequency of the loss maximum, and  $A$ ,  $B$ , and  $T_0$  are adjustable parameters. It was revealed previously for solutions of PS, PVAC, and PVCL that the value of the parameters  $A$  and  $B$  are almost independent of concentration above 50%.<sup>1-3</sup> The parameters determined from best-fit curves for the present system are listed in Table I. As described in ref 1,  $A$  and 2.3 RB are respectively the logarithm of the relaxation energy and the activation energy at an infinite temperature where the molecular motions are fully activated and may be independent of intermolecular interactions. Therefore, these parameters are considered to be intrinsic to the polymer and independent of concentration. In contrast to previous results, parameters  $A$  and  $B$  varied appreciably with concentration. This, however,

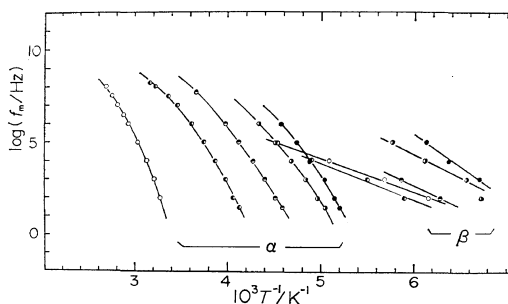


Figure 9. Activation plots for the  $\alpha$  and  $\beta$  processes: ●, 30%; ○, 45%; ◐, 60%; ◑, 75%; ○, 100%.

might be ascribed to the apparent shift of the loss peak temperature, as the  $\alpha$  and  $\beta$  peaks overlap each other.

#### Activation Energy for the $\beta$ Process

The activation plots for the  $\beta$  process are shown in Figure 9. The activation energies determined from the slope of the plots are shown in Figure 10. In the systems PS-TOL and PVAC-TOL, the activation energy for the secondary relaxation process was about 130 kJ/mol at 30% concentration. In this system, the activation energy for the  $\beta$  process is considerably smaller than 130 kJ/mol. Obviously this can be attributed to the difference in the origin of the process. The activation energy varied step-wise at a concentration of about 70%. This fact seems to correlate with the fact that concentration dependence of the peak temperature changed at about 70% as can be seen in Figure 3. The decrease of the activation energy with increasing concentration may be unusual. Cooperative motion of the side group and the solvent molecule would explain this fact.

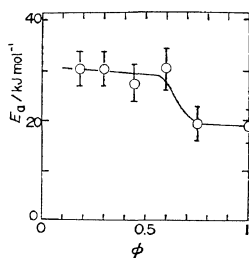


Figure 10. Activation energies for the  $\beta$  process;  $\phi$ , weight fraction of the PMA.

#### Glass Transition

Glass transition temperatures determined by DTA measurements are plotted in Figure 11 together with the temperatures  $T_D$  where dielectric relaxation times for the  $\alpha$  and  $\beta$  processes are 100 s. Below 30%, two step-wise changes were recognized in the DTA diagram as shown in Figure 12. They are designated as glass transitions,  $T_{gI}$  and  $T_{gII}$  in the order of decreasing temperature. Similar behavior was also observed in the PVAC-TOL system. As shown in Figure 11,  $T_{gI}$  and  $T_{gII}$  correspond respectively to the  $\alpha$  and  $\beta$  processes. Therefore we can conclude that segmental motion is frozen-in at  $T_{gI}$  but the

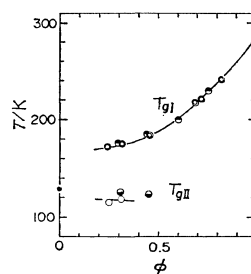


Figure 11. Glass transition temperatures determined by DTA and the temperature ( $T_D$ ) where dielectric relaxation time is 100 s:  $\odot$ ,  $T_{gI}$ ;  $\circ$ ,  $T_{gII}$ ;  $\bullet$ ,  $T_D$  for the  $\alpha$  process;  $\ominus$ ,  $T_D$  for the  $\beta$  process.

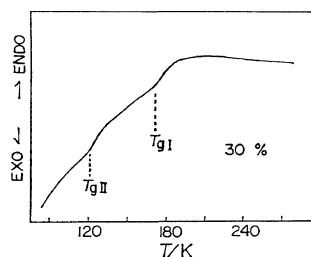


Figure 12. DTA diagram for the solution with the concentration of 30%. The heating rate was 7 K/min.

motions of the side group or the solvent are frozen-in at  $T_{gII}$ .

#### Shape of the Frequency Dependence Curve of $\epsilon''$

As can be seen in Figures 6, 7, and 8, the loss peaks of the  $\alpha$  and  $\beta$  processes coalesce with increasing temperature. At the same time, the loss curve of the  $\beta$  process narrows. For example, the half width of the loss curve of the  $\beta$  process for the 45% solution is about 6 decades at 182 K whereas it decreases to 4 decades at 243 K. It should be noted that when segmental motion is more rapid than the rotation of the side group, the loss due to rotation of the side group in terms of dielectric method cannot be observed since the rate of motion of the side group is governed by the segmental motion of the backbone. It may be expected in the present system that this situation occurs with an increase in temperature since the activation plots for the  $\alpha$  and  $\beta$  processes intersect with each other as shown in Figure 9. Therefore the change of the shape of the loss curve may be explained by examining temperature dependences of the auto-correlation functions of the dipole

$\phi_\alpha(t)$  and  $\phi_\beta(t)$  for the  $\alpha$  and  $\beta$  processes where  $t$  denotes time. We also define the auto-correlation function  $\phi_\beta(t)$  for motion of the side group with respect to the coordinate fixed on the backbone. This function is the correlation function when segmental motion ceases and hence corresponds to the correlation function below  $T_g$ . Then the function  $\phi_\beta(t)$  may be written in the form

$$\phi_\beta(t) = \phi_\alpha(t)\phi_\beta(t) \quad (5)$$

Cook, *et al.*,<sup>10</sup> expressed  $\phi_\alpha(t)$  as

$$\phi_\alpha(t) = \exp[-(t/\tau_\alpha)^{\bar{a}}] \quad (6)$$

where  $\tau_\alpha$  is a constant corresponding to the relaxation time and  $\bar{a}$  is a parameter with a value of about 0.5 for ordinary amorphous polymers. They reproduced the non-symmetrical loss curve for the primary process using the function. The shape of the loss curve for the  $\beta$  process is nearly symmetrical with respect to the logarithm of frequency. Assuming a Gaussian distribution of relaxation times  $\tau$  with respect to  $\ln \tau$ , Wagner<sup>11</sup> represented a decay curve of polarization  $\psi$  as

$$\psi(t) = (\bar{b}/\sqrt{\pi}) \int_{-\infty}^{\infty} \exp[-\bar{b}^2 z^2 - (t/\tau_0) \exp(-z)] dz \quad (7)$$

where  $\bar{b}$  is a constant which represents broadness of distribution of relaxation time and  $\tau_0$  and  $z$  denote the average relaxation time and  $\ln(\tau/\tau_0)$  respectively. We use this function for  $\phi_\beta(t)$  replacing  $\tau_0$  by  $\tau_\beta$ . Assuming that the cross correlation functions between dipoles can be ignored and that the microscopic correlation function is the same as the macroscopic decay function of the polarization  $F(t)$ , we have calculated the frequency dependence of  $\epsilon''$  in terms of Fourier transformation of  $\dot{F}(t)$  which is given by

$$\dot{F}(t) = \Delta\epsilon_\alpha \dot{\phi}_\alpha(t) + \Delta\epsilon_\beta \dot{\phi}_\beta(t) \quad (8)$$

where a dot indicates differentiation with time. This calculation was performed by means of an

electronic computer. The values of  $\tau_\alpha$  and  $\tau_\beta$  are expressed by the Vogel and the Arrhenius equations which conform to the experimental activation plot with the relaxation time relation given by  $(2\pi f_m)^{-1}$ . The parameter  $\bar{a}$  and  $\bar{b}$  in eq 6 and 7 are taken to be 0.5 and 0.25, respectively. The values of  $\Delta\epsilon_\alpha$  and  $\Delta\epsilon_\beta$  above  $T_g$  were used ignoring temperature dependence. The results of the calculation are shown for the 45-% solution and the bulk PMA in Figures 6 and 8. As can be seen, the results agree fairly well with the loss curves observed. Therefore the temperature dependence of the shape of the loss curve is explained in terms of this model. However, the calculated values and the experimental values do not agree quantitatively. This disagreement may be due to the approximations mentioned above particularly, the approximation of the complete independence of  $\phi_\alpha$  and  $\phi_\beta$ .

#### REFERENCES

1. K. Adachi, I. Fujihara, and Y. Ishida, *J. Polym. Sci., Polym. Phys. Ed.*, **13**, 2155 (1975).
2. K. Adachi and Y. Ishida, *J. Polym. Sci., Polym. Phys. Ed.*, **14**, 2219 (1976).
3. K. Adachi, M. Hattori, and Y. Ishida, *J. Polym. Sci., Polym. Phys. Ed.*, **15**, 693 (1977).
4. N. G. McCrum, B. E. Read, and G. Williams, "Anelastic and Dielectric Effects in Polymeric Solids," John Wiley, New York, N. Y., 1967.
5. G. P. Mikhailov, T. I. Borisova, and D. A. Dmitrochenko, *J. Tech. Phys. (USSR)*, **26**, 1924 (1956).
6. K. Adachi, Y. Hirose, and Y. Ishida, *J. Polym. Sci., Polym. Phys. Ed.*, **13**, 737 (1975).
7. C. P. Smyth, "Dielectric Behavior and Structure," McGraw-Hill, New York, N. Y., 1955.
8. H. Vogel, *Phys. Z.*, **22**, 645 (1921).
9. G. Tamman and W. Hesse, *Z. Anorg. Allgem. Chem.*, **156**, 245 (1926).
10. M. Cook, D. C. Watts, and G. Williams, *Trans. Faraday Soc.*, **66**, 2503 (1970).
11. K. W. Wagner, *Ann. Phys.*, **40**, 817 (1913).